10. P. M. DiGrazia *et al.*, unpublished results.
11. The chemostat operating conditions were as follows: temperature, 25°C; dilution rate, 0.4 hour^{-1}; mean cell residence time, 2.5 hours. Feed consisted of a minimal salts medium (*3*) containing sodium succinate (100 mg liter^{-1}), yeast extract (100 mg liter^{-1}), and tetracycline (14 mg liter^{-1}); naphthalene was added to one of the two feed supplies at 30 mg liter^{-1}.
12. K. Truong and J. W. Blackburn, *Environ. Prog.* **3**, 143 (1984).
13. The MGP soil was obtained from a site in the northeastern United States. The total PAH concentration was 3227 mg kg^{-1}, of which 1240 mg kg^{-1} was naphthalene. An uncontaminated Etowah soil obtained from East Tennessee was used as the control soil.
14. A. V. Ogram, G. S. Sayler, T. Barkay, *J. Microbiol. Methods* **7**, 57 (1987); G. S. Sayler, J. Fleming, B. Applegate, C. Werner, K. Nikbakht, in *Recent Advances in Microbial Ecology*, T. Hattori, Y. Ishida, Y. Maruyama, R. Y. Morita, A. Uchida, Eds. (Japan Scientific Societies Press, Tokyo, 1989), pp. 658–662.
15. Supported by the U.S. Geological Survey, Office of Water Research grant 14-08-0001-G1482, U.S. Air Force contract F49620-89-C-0023, Gas Research Institute contract 5087-253-1490, Electric Power Research Institute contract RP-3015-1, the University of Tennessee, Waste Management Research and Education Institute, and IT Corporation.

30 March 1990; accepted 8 June 1990

Antibody-Catalyzed Porphyrin Metallation

ANDREA G. COCHRAN AND PETER G. SCHULTZ*

An antibody elicited to a distorted *N*-methyl porphyrin catalyzed metal ion chelation by the planar porphyrin. At fixed Zn^{2+} and Cu^{2+} concentrations, the antibody-catalyzed reaction showed saturation kinetics with respect to the substrate mesoporphyrin IX (2) and was inhibited by the hapten, *N*-methylmesoporphyrin IX (1). The turnover number of 80 hour^{-1} for antibody-catalyzed metallation of 2 with Zn^{2+} compares with an estimated value of 800 hour^{-1} for ferrochelatase. The antibody also catalyzed the insertion of Co^{2+} and Mn^{2+} into 2, but it did not catalyze the metallation of protoporphyrin IX (3) or deuteroporphyrin IX (4). The antibody has high affinity for several metalloporphyrins, suggesting an approach to developing antibody-heme catalysts for redox or electron transfer reactions.

THE IMMUNE SYSTEM PRODUCES A repertoire of 10^{10} to 10^{12} antibody molecules (*1*) that can recognize and bind a huge array of naturally occurring and synthetic molecules. Recently, the tremendous diversity and specificity of the immune response have been merged with our understanding of chemical processes to produce catalytic antibodies. Since the first reports of antibody catalysis (*2*), a wide variety of transformations have been examined (*3*). In addition, several general strategies have been developed for the rational design of catalytic antibodies. We report the generation of antibodies to a hapten that mimics a strained conformation of substrate. Antibodies specific for a distorted *N*-methyl porphyrin catalyze metal ion chelation by the corresponding planar, non-methylated porphyrin. This system expands the catalytic antibody repertoire to include ligand substitution reactions.

Ferrochelatase, the terminal enzyme in the heme biosynthetic pathway, catalyzes the insertion of Fe^{2+} into protoporphyrin IX (**3**) (*4*). *N*-methyl-protoporphyrin IX is a potent inhibitor of ferrochelatase with an inhibition constant (K_i) of 7 nM (*5*). The distortion of the porphyrin macrocycle resulting from *N*-alkylation is thought to approximate the transition state of the enzymatic reaction (*4, 6*). Such bending would increase exposure of the pyrrole nitrogen lone pairs to solvent and thus facilitate metal ion complexation. Indeed, kinetic studies have shown that *N*-alkylporphyrins chelate metal ions 10^3- to 10^5-fold faster than their non-alkylated cognates (*4*). We reasoned that if *N*-methylporphyrins are in fact transition state analogs for porphyrin metallation, antibodies elicited to such compounds should catalyze metal ion incorporation by distortion of the corresponding substrate.

We prepared antibodies specific for *N*-methylmesoporphyrin IX (**1**) (isomer mixture, Porphyrin Products, Inc., Logan, Utah) (Fig. 1). We chose **2** as substrate rather than **3** because of the relative photosensitivity of the latter (*7*) and the greater tendency of **3** to aggregate in aqueous solution (*8*). In addition, several convenient ferrochelatase assays have been described that use mesoporphyrin as substrate (*9–11*). Three hybridoma lines were identified that produced antibodies specific for **1** (*12*). Two of the three purified antibodies catalyzed Zn(II) and Cu(II) mesoporphyrin formation. The faster of these, 7G12-A10-G1-A12, was characterized further (*13*).

The antibody-catalyzed reaction could be described by the following scheme:

$$\mathrm{Ig} + \mathrm{S} \overset{K_m}{\rightleftharpoons} \mathrm{Ig \cdot S} \xrightarrow[M^{2+}]{k_{cat,app}} \mathrm{Ig \cdot P} \overset{K_p}{\rightleftharpoons} \mathrm{Ig} + \mathrm{P}$$

where S is porphyrin substrate, P is metalloporphyrin product, M^{2+} is metal, Ig is antibody, K_m is the Michaelis constant, K_p is the product inhibition constant, and $k_{cat,app}$ is the k_{cat} (catalytic constant) observed with a particular fixed concentration of metal. Significant product inhibition by Zn(II) mesoporphyrin and the relative inaccuracy of the assay at small percentages of substrate conversion did not allow the determination of initial rates for this reaction. The data were therefore fit to the integrated form of Eq. 1 (*14*):

$$\frac{d[P]}{dt} = \frac{V_{max,app}[S]}{K_m(1 + [P]/K_p) + [S]} \quad (1)$$

Typical plots for different porphyrin concentrations at 1 mM Zn^{2+} are shown in Fig. 2 [K_m = 49 μM, K_p = 2.9 μM, and $V_{max,app}$ (maximum apparent velocity) = 24 μM hour^{-1}]. The pseudo first-order rate constant for uncatalyzed metallation at the same Zn^{2+} concentration is 0.031 hour^{-1}. Chelation of Co^{2+} and Mn^{2+} was also catalyzed, but because of the much greater product inhibition and substantially slower reaction rates, no further kinetic characterization was attempted. Incorporation of Ni^{2+} was not catalyzed.

Copper(II) mesoporphyrin was not observed to inhibit antibody catalysis up to concentrations of at least 15 μM, allowing the determination of initial rates for production of this metalloporphyrin. A Lineweaver-Burk plot for antibody-catalyzed Cu^{2+} incorporation (1 mM Cu^{2+}) gives a K_m for **2** of 50 μM, nearly identical to the value obtained with Zn^{2+}, and a $V_{max,app}$ of 2.6 μM hour^{-1} (Fig. 3). The pseudo first-

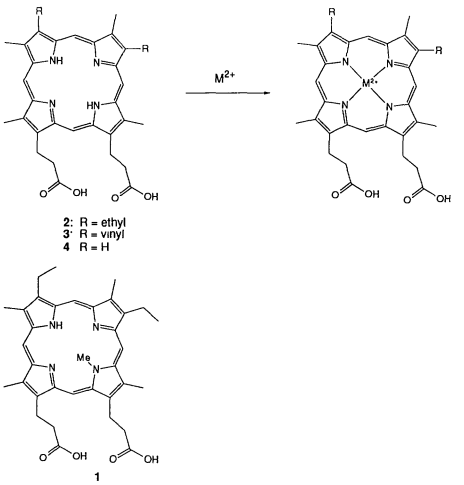

Fig. 1. Hapten and reaction scheme for metalloporphyrin formation.

Department of Chemistry, University of California, Berkeley, CA 94720.

*To whom correspondence should be addressed.

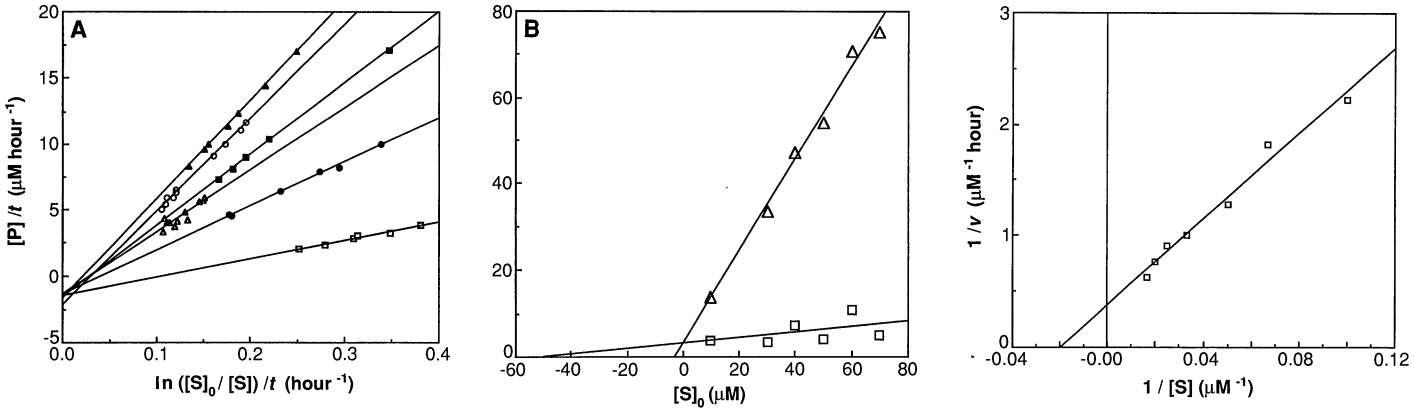

Fig. 2. (**A**) Plot of $[P]/t$ as a function of $[\ln([S]_0/[S])]/t$ for various concentrations of **2** at 1 mM Zn^{2+}. Concentrations of **2** are 70 (▲), 60 (○), 50 (■), 40 (△), 30 (●), and 10 μM (□). (**B**) Replot of data in (A). Slope (△) or slope − $[S]_0$ (□) is shown as a function of initial substrate concentration. The x-intercepts are $-K_p$ and $-K_{m,app}$, respectively; $V_{max,app}$ is obtained from the y-intercept of (A).

Fig. 3. Lineweaver-Burk plot of antibody-catalyzed Cu(II) mesoporphyrin formation at 1 mM Cu^{2+}.

order rate constant for uncatalyzed Cu^{2+} chelation (1 mM Cu^{2+}) is 0.005 $hour^{-1}$. Antibody activity was examined as a function of Cu^{2+} concentration. No evidence of saturation of antibody by metal was observed between 0.5 and 2.5 mM Cu^{2+}, suggesting that binding of metal ions by antibody does not contribute significantly to catalysis.

Catalytic activity was effectively inhibited by addition of stoichiometric amounts of hapten **1**. Various metalloporphyrins also inhibited the reaction (Table 1). Interestingly, the inhibition by metal(III) mesoporphyrins [Mn(III) and Fe(III)] is markedly greater than inhibition by divalent metal mesoporphyrins [Zn(II) and Cu(II)]. *N*-alkyl, non-mesotetraarylporphyrins are protonated at physiological pH (*6*). Metalloporphyrins with more positive-charge density at the metal center may mimic more closely the positively charged hapten. Antibodies elicited to Fe(III) and Co(III) *meso*-tetrakis(4-carboxyphenyl)porphine have been reported by Schwabacher and coworkers to discriminate various metal complexes of this porphyrin (*15*).

Some variation in porphyrin structure is tolerated by the antibody, as the Fe(III) chelates of **3** and deuteroporphyrin IX (**4**) inhibit antibody catalysis of Zn(II) mesoporphyrin formation. We therefore examined **3** and **4** as possible substrates for the antibody. Surprisingly, no rate enhancements were observed within experimental error (*16*). These porphyrins may not bind productively to antibody. In contrast, ferrochelatase efficiently metallates all three of these porphyrins (*5*). Such finely tuned substrate specificities have frequently been observed in antibody catalysis.

Several properties of the antibody are similar to those of the enzyme ferrochelatase. Reported ferrochelatase K_m values for **2**, **3**, and **4** are typically between 10 and 70 μM (*4, 5, 17, 18*), compared to 50 μM for the antibody. Product inhibition is observed with enzyme as well as antibody; reported enzyme K_i values range from 1 to 10 μM for those metal(II) porphyrins tested (*4, 5*). In addition, it appears likely (Table 1) that antibody-hapten affinity is comparable to the affinity of ferrochelatase for *N*-methylprotoporphyrin. The enzyme readily utilizes both Fe^{2+} and Zn^{2+} as substrates, and shows some activity with Co^{2+} and Ni^{2+} (*4, 18*), but Mn^{2+}, Cu^{2+}, and Mg^{2+} are not incorporated. The antibody, however, incorporates Zn^{2+}, Cu^{2+}, Co^{2+}, and Mn^{2+}. The failure of antibody to catalyze the formation of Ni(II) porphyrins is most likely due to the combination of the slow ligand-exchange kinetics of Ni^{2+} and the use of a reaction buffer (tris) that complexes metal ions. No background reaction was observed with this metal ion.

Table 1. Porphyrin specificity of antibody. Percent inhibition (%I) of antibody-catalyzed Zn^{2+} insertion into mesoporphyrin was determined at 300 nM and 1 μM inhibitor. Inhibition was assayed spectrophotometrically at 570 nm with a Kontron Instruments Uvikon 860 UV-visible spectrophotometer. Reaction mixtures contained 60 μM **2**, 1 mM Zn(II) acetate, inhibitor, and 0.3 μM antibody. Other reaction conditions were as described above (*13*).

Porphyrin	%I, 300 nM	%I, 1 μM
N-methylmesoporphyrin (**1**)	40	100
Mn(III) mesoporphyrin	40	100
Fe(III) mesoporphyrin	40	90
Zn(II) mesoporphyrin	0	10
Fe(III) protoporphyrin	40	80
Fe(III) deuteroporphyrin	20	40

The rate of antibody-catalyzed metalloporphyrin synthesis can be compared to the enzyme-catalyzed and background rates. On the basis of a molecular weight of 40 kD for the enzyme and reported V_{max} values for purified bovine ferrochelatase (Fe^{2+} insertion) (*5*), turnover numbers of 252, 588, and 2640 $hour^{-1}$ for **3**, **2**, and **4**, respectively, can be calculated. This enzyme has a specific activity with Zn^{2+} that is 136% of the Fe^{2+} activity (*18*). From the above k_{cat} for **2** an approximate Zn^{2+} value of 800 $hour^{-1}$ can be calculated. From the antibody $V_{max,app}$, a $k_{cat,app}$ value of at least 80 $hour^{-1}$ at 1 mM Zn^{2+} is obtained based on total antibody. The enzyme can achieve maximal turnover with substantially less metal (K_m = 32 μM) (*18*) than the amount present in the antibody assay; however, the antibody has not reached a maximum rate. A rate enhancement for antibody-catalyzed versus background metallation can be obtained from the ratio of antibody k_{cat} to the background pseudo first-order rate constant at the same metal concentration. These values are 2600 and 1700 for Zn^{2+} and Cu^{2+} insertion, respectively, at 1 mM metal salt.

These studies suggest that *N*-alkyl porphyrins are indeed appropriate transition-state analogs for porphyrin metallation. Additionally, this antibody may provide a simple model system for the study of porphyrin metallations in water. Although we do not yet have any direct evidence of a porphyrin conformational change upon binding to antibody (*19*), spectroscopic or crystallographic studies and measurement of the energy barrier for distortion of **2** (*20*) may clarify this point. The ability to obtain antibodies specific for natural porphyrins should undoubtedly facilitate development of antibody-porphyrin complexes to mimic the rich chemistry of heme proteins.

REFERENCES AND NOTES

1. T. Honjo and S. Habn, *Annu. Rev. Biochem.* **54**, 803 (1985).
2. A. Tramontano, K. D. Janda, R. A. Lerner, *Science* **234**, 1566 (1986); S. J. Pollack, J. W. Jacobs, P. G. Schultz, *ibid.*, p. 1570.
3. For reviews, see P. G. Schultz, R. A. Lerner, S. J. Benkovic, *Chem. Eng. News* **68**, 26 (1990); K. M. Shokat and P. G. Schultz, *Annu. Rev. Immunol.* **8**, 335 (1990); P. G. Schultz, *Angew. Chem. Int. Ed.*

Engl. **28**, 1283 (1989); *Acc. Chem. Res.* **22**, 287 (1989).
4. D. K. Lavallee, *Mol. Struct. Energ.* **9**, 279 (1988).
5. H. A. Dailey and J. E. Fleming, *J. Biol. Chem.* **258**, 11,453 (1983).
6. D. K. Lavallee, *The Chemistry and Biochemistry of N-Substituted Porphyrins* (VCH, New York, 1988).
7. F. R. Hopf and D. G. Whitten, in *The Porphyrins*, D. Dolphin, Ed. (Academic Press, New York, 1978), vol. 2, pp. 161–195.
8. W. I. White, *ibid.*, vol. 5, pp. 303–339.
9. F. Li, C. K. Lim, T. J. Peters, *Biomed. Chromatogr* **2**, 164 (1987).
10. R. G. Roberts, *ibid.*, **2**, 71 (1987).
11. E. Rossi, K. A. Costin, P. Garcia-Webb, *Clin. Chem.* **34**, 2481 (1988).
12. Carrier proteins bovine serum albumin and ovalbumin were treated with the *bis-N*-hydroxysuccinimide ester of hapten **1**. Epitope densities ranged from five to ten haptens per carrier monomer. Swiss-Webster mice were immunized, and spleen cells were fused with the myeloma line SP 2/0. Binding of these antibodies to hapten-protein conjugates was completely inhibited by preincubation of cell culture supernatants with 50 μg/ml (86 μM) free hapten. Antibodies [immunoglobulin G1 (IgG1)] were purified from ascites fluid by Protein A affinity chromatography and were determined to be >95% IgG by denaturing polyacrylamide gel electrophoresis [U. Laemmli, *Nature* **227**, 680 (1970)]. Protein concentrations were determined by Bradford assay [M. M. Bradford, *Anal. Biochem.* **72**, 248 (1976)] and by absorbance at 280 nm.
13. Reactions were assayed (*9*) by reversed-phase high-performance liquid chromatography with a Hewlett-Packard Model 1190L Liquid Chromatograph equipped with a Waters Associates Model 625 Diode-Array Detector, a Hewlett-Packard Model 3396A Integrator, and a Dynamax C18 column (4.6 mm by 25 cm, 5-μm particle size, Rainin Instruments). Mobil phase consisted of 0 to 15% 1 M ammonium acetate, pH 5.2, in methanol. Various isocratic or gradient elutions were performed depending on the retention characteristics of the particular porphyrins in the mixture. Detection was at 390 nm for Cu(II) mesoporphyrin, 370 nm for Mn(III) mesoporphyrin, 410 nm for Co(III) mesoporphyrin, 420 nm for Co(III) protoporphyrin, and 400 nm for all other porphyrins. Reaction aliquots (40 μl) were mixed with 160 μl of 30% dimethylsulfoxide (DMSO) (v/v) in methanol containing 1 to 5 μM of an appropriate metalloporphyrin as an internal standard. After filtration, this mixture was directly injected onto the column. Plots of product: internal standard area ratios versus product concentration were linear for solutions containing up to 40 μM product. Reaction mixtures (300 μl) contained porphyrin, metal salt, 90 mM tris acetate, pH 8.0, 0.5% (w/v) Triton X-100, and 5% (v/v) DMSO. Antibody reactions additionally contained 50 μg of protein per milliliter (0.3 μM). Reactions were incubated at 26°C.
14. I. H. Segel, *Enzyme Kinetics* (Wiley-Interscience, New York, 1975), pp. 59–61.
15. A. W. Schwabacher, M. I. Weinhouse, M.-T. M. Auditor, R. A. Lerner, *J. Am. Chem. Soc.* **111**, 2344 (1989).
16. Deuteroporphyrin metallation was assayed with Zn^{2+}. Protoporphyrin metallation was assayed with Cu^{2+} and Co^{2+}.
17. S. Taketani and R. Tokunaga, *J. Biol. Chem.* **256**, 12,748 (1981).
18. ———, *Eur. J. Biochem.* **127**, 443 (1982).
19. The ultraviolet-visible spectrum of mesoporphyrin (10 μM) in reaction buffer was compared to the spectrum in the presence of excess antibody. A slight red-shift of 1 to 2 nm (397 to 398 nm, Soret band) was detected upon binding to antibody. No change was observed in the relative positions or intensities of the visible bands. In particular, the spectrum bore no similarity to that of the hapten.
20. R. F. Pasternack, N. Sutin, D. H. Turner, *J. Am. Chem. Soc.* **98**, 1908 (1976).
21. We thank P. R. Ortiz de Montellano for helpful discussions and R. Ranon for production of antibodies. Financial support was provided by Affymax Research Institute, the Office of Naval Research (ONR N0014-87-K-0256), an NSF Waterman Award (CHE-8451306) to P.G.S., and by Schering-Plough to A.G.C.

2 May 1990; accepted 28 June 1990

External Guide Sequences for an RNA Enzyme

ANTHONY C. FORSTER AND SIDNEY ALTMAN*

Ribonuclease P (RNase P) from *Escherichia coli* or its catalytic RNA subunit can efficiently cleave small RNA substrates that lack the conserved features of natural substrates of RNase P if an additional small RNA is also present. This additional RNA must contain a sequence complementary to the substrate [external guide sequence (EGS)] and a 3′-proximal CCA sequence to ensure cleavage. The aminoacyl acceptor stem and some additional 5′- and 3′-terminal sequences of a precursor transfer RNA are sufficient to allow efficient cleavage by RNase P, and the 2′-hydroxyl group at the cleavage site is not absolutely necessary for cleavage. In principle, any RNA could be targeted by a custom-designed EGS RNA for specific cleavage by RNase P in vitro or in vivo.

ALL REACTIONS THAT ARE GOVerned by RNA in vivo result in the transesterification or hydrolysis of specific phosphodiester bonds in RNA. In several classes of these reactions, an intramolecular site of cleavage or ligation is identified by internal guide sequences (IGSs) which form base pairs with the segment of the phosphodiester chain that contains the cleavage site (*1*). However, IGSs are not present in the class of reactions governed by RNA that are enzymatic in vivo, namely, the cleavage of precursor tRNA molecules by the RNA component of eubacterial RNase P (*2, 3*). The nucleotide sequence of the segment of the phosphodiester chain that contains the cleavage site is not conserved among different substrates for RNase P (*4*), so it cannot be recognized by a unique IGS in the enzyme. We propose that the 3′-proximal sequence of the acceptor stem of a precursor tRNA can be regarded as an "external guide sequence" (EGS; Fig. 1A) because it identifies the site of cleavage, in part, by forming base pairs with the segment of the phosphodiester chain that is cleaved. In contrast to IGSs, which are covalently attached to a "catalytic" sequence in vivo, EGSs are external to the native enzyme and are highly variable. We show that an EGS is essential for cleavage of a substrate by RNase P from *E. coli* and that the EGS is still functional when detached from the substrate. We have used EGS-containing RNAs (EGS RNAs) to construct a very small model substrate for RNase P and to investigate the mechanism of recognition and cleavage of the substrate. Furthermore, we propose that any RNA may be targeted for specific cleavage in vitro or in vivo by RNase P provided that the RNA is associated with a custom-designed EGS RNA.

The importance of the EGS for cleavage by RNase P was tested with derivatives of the smallest model substrate reported to be cleaved efficiently by RNase P, pAT1 [Fig. 1B; (*5*)]. As anticipated from previous work (*5*), derivatives of pAT1 with 3′-terminal truncations that deleted the EGS, termed Hinf I pAT1 and Taq I pAT1 [these RNAs consist of the 5′-terminal 24 and 31 nucleotides (nt) of pAT1, respectively; Fig. 1B], were not cleaved by RNase P from *E. coli* (M1 RNA plus C5 protein) or by M1 RNA under conditions where pAT1 was cleaved efficiently (Fig. 2, lanes 1 through 4; pAT1, Hinf I pAT1, and Taq I pAT1 are represented by P, H, and T, respectively). However, if an RNA that contained the deleted EGS [either the 29-nt EGS RNA or the 20-nt EGS RNA (Fig. 1, C and D)] was added to the reaction mixture, Hinf I pAT1 and Taq I pAT1 were cleaved efficiently at the same cleavage site as in pAT1 (Fig. 2, lanes 6, 7, 9, and 10). The 20- and 29-nt EGS RNAs did not stimulate the cleavage of pAT1 by M1 RNA or RNase P (Fig. 2, lanes 2, 5, and 8). In addition, a 17-nt RNA, designed such that a substrate and an EGS RNA could be made from the same sequence (Fig. 1E), was also cleaved efficiently by RNase P (Fig. 2B, lanes 11 and 12), but was cleaved poorly by M1 RNA (Fig. 2A, lanes 11 and 12). Although the 17-nt RNA contains the same octanucleotide 3′-terminal sequence as the 20- or 29-nt EGS RNAs, Hinf I pAT1 and Taq I pAT1 were not cleaved by M1 RNA or by RNase P in the presence of the 17-nt RNA, indicating that the functions of the 20- and 29-nt EGS RNAs were not just

Department of Biology, Yale University, New Haven, CT 06520.

*To whom correspondence should be addressed.